J|A|C|S
ARTICLES
Published on Web 12/06/2006

Hsc70 ATPase: An Insight into Water Dissociation and Joint Catalytic Role of K^+ and Mg^{2+} Metal Cations in the Hydrolysis Reaction

Mauro Boero,*[,†] Takashi Ikeda,[‡] Etsuro Ito,[§,||] and Kiyoyuki Terakura[||,⊥]

Contribution from the Center for Computational Sciences, University of Tsukuba, Tennodai 1-1-1, Tsukuba, Ibaraki 305-8577, Japan and CREST, Japan Science and Technology Agency, 4-1-8 Honcho, Kawaguchi, Saitama 332-0012, Japan, Synchrotron Radiation Research Unit, Quantum Beam Science Directorate (QuBS), Japan Atomic Energy Agency (JAEA), Hyogo 679-5148, Japan, Faculty of Pharmaceutical Sciences at Kagawa Campus, Tokushima Bunri University, Shido 1314-1, Sanuki 769-2193, Japan, Division of Frontier Research, Creative Research Initiative "Sousei", Hokkaido University, Kita 21-Nishi 10, Sapporo 001-0021, Japan, and Research Institute for Computational Sciences, National Institute of Advanced Industrial Science and Technology, 1-1-1 Umezono, Tsukuba, Ibaraki 305-8568, Japan

Received June 11, 2006; E-mail: boero@comas.frsc.tsukuba.ac.jp

Abstract: Hybrid quantum mechanics/molecular mechanics simulations, coupled to the recently introduced metadynamics method, performed on the adenosine triphosphate (ATP) of the bovine Hsc70 ATPase protein, show which specific water molecule of the solvation shell of the Mg^{2+} metal cation acts as a trigger in the initial phase of the ATP hydrolysis reaction in ATP synthase. Furthermore, we provide a detailed picture of the reaction mechanism, not accessible to experimental probes, that allows us to address two important issues not yet unraveled: (i) the pathway followed by a proton and a hydroxyl anion, produced upon dissociation of a putative catalytic H_2O molecule, that is crucial in the selection of the reaction channel leading to the hydrolysis; (ii) the unique and cooperative role of K^+ and Mg^{2+} metal ions in the reaction, acting as cocatalysts and promoting the release of the inorganic phosphate via an exchange of the OH^- hydroxyl anion between their respective solvation shells. This is deeply different from the proton wire mechanism evidenced, for instance, in actin and lowers significantly the free energy barrier of the reaction.

1. Introduction

The 70-kDa heat shock protein (Hsp70) family is a higly conserved, ubiquitous group of proteins that plays a fundamental role in protecting cells from stress. The name comes from its first observation as a response to heat shock and has a wealth of roles.[1] Namely, Hsp70 serves as an indicator for cellular stress as a molecular chaperone, plays a pivotal role in maintaining cellular homeostasis by preventing apoptosis, influences energy metabolism, facilitates cellular processes in terms of muscular adaptation, and interacts with other signalling pathways (for a review see ref 1 and references therein). All members of the family have an ATPase activity, which regulates cycles of binding and release from unfolded proteins, although the exact mechanism is still unclear.

Heat shock cognate (Hsc70) protein is a mammalian member of this family originally described as a *clathrin-uncoating protein*.[2] The molecular structure of Hsp70 comprises three parts:[1−3] N-terminal adenosin-triphosphate (ATP) synthase (ATPase) domain, peptide-binding site, and C-terminus (see, e.g., Figure 1 of ref 1). The crystal structure of the 44-kDa ATPase domain has been solved, and the tertiary fold turned out to be similar to that of actin which is also an ATPase.[3] Furthermore it is similar to two other phosphotransferases, namely hexokinase and glycerol kinase. The ATPase reaction is of fundamental importance in all organisms and has been defined as "the principal net chemical reaction occurring in the whole world" by P. D. Boyer in his Nobel Lecture.[4] The main phases consist in an attack of an H_2O molecule to ATP that, upon water dissociation, releases a terminal phosphate group and reverts to ADP with a general reaction mechanism summarized as $ATP + H_2O \rightarrow ADP + P_i$. This transformation of triphosphate into diphosphate (ADP) occurs in the presence of metal ions (Mg^{2+}/Ca^{2+}, K^+) located in close proximity of the phosphate chain, and these cations play a catalytic role that has not yet been completely understood and for which a general consensus has not yet been reached.[5−14] At variance with other

† University of Tsukuba and CREST.
‡ Japan Atomic Energy Agency (JAEA).
§ Tokushima Bunri University.
|| Hokkaido University.
⊥ National Institute of Advanced Industrial Science and Technology.

(1) Liu, Y.; Gampert, L.; Nething, K.; Steinacker, J. M. *Frontiers Biosci.* **2006**, *11*, 2802−2827.
(2) Chapell, T. G.; Welch, W. J.; Schlossman, D. M.; Palter, K. B. Schlesinger, M. J.; Rothman, J. E. *Cell* **1986**, *45*, 3−13.
(3) Flaherty, K. M.; DeLuca-Flaherty, C.; McKay, D. B. *Nature* **1990**, *346*, 623−628.
(4) Boyer, P. D. In *Nobel Lectures, Chemistry 1996*−2000; Grenthe, I., Ed.; World Scientific Publishing: Singapore, 2003; p 120.
(5) Boyer, P. D. *Annu. Rev. Biochem.* **1997**, *66*, 717−749.
(6) Pollard, T. D. *Mol. Biol. Cell* **2004**, *15*, 11A.

10.1021/ja064117k CCC: $33.50

systems,[15−17] it has been shown that in the ATPase activity of Hsc70, K^+ has a central role. In particular both K^+ and Mg^{2+} are required for the dissociation of denatured proteins from the *E. coli* homologue of Hsc70. Moreover Na^+ does not substitute for the K^+ cation.[18,19] Despite structural homologies with Hsc70, this represents a basic difference with respect to actin, where potassium cations are not present and, in particular, the K_1^+ site is replaced by the ϵ-amino group of lysine.[20,21]

Clearly an atomistic detailed computer simulation of the system could greatly help in understanding the role of the potassium ion, since a detailed microscopic picture escapes any experimental probe. For such large biomolecules, realistic simulations able to be treated with sufficient accuracy are becoming possible only now[8,10,22−26] thanks to the development of computational resources and numerical algorithms. Yet several questions are still unanswered, and, as acknowledged, for instance, by the authors of the most recent computational work on actin,[23] an adequate dynamical treatment of the whole system via hybrid quantum mechanics/molecular mechanics (QM/MM) simulations coupled to a suitable method for reaction path sampling is still lacking. Conventional molecular dynamics would require an unfeasible amount of time to generate reactive trajectories whenever activation barriers are larger than k_BT ($\sim$0.6 kcal/mol at $T = 300$ K, k_B being the Boltzmann constant). Furthermore, most of the classical biomolecular force fields are unable to model any reactive process due to the harmonic potential for bond stretch. For these reasons, in the present work, we sample the ATP-to-ADP reaction path in Hsc70 protein via QM/MM simulations coupled with the recently introduced metadynamics method,[27,28] capable of efficiently exploring the free energy surface (FES) of complex chemical and biochemical reactions and providing a microscopic insight into reaction pathways within affordable simulation times. The target of our study is a fully solvated bovine Hsc70 ATPase system, that has been extensively investigated experimentally[1−3,12,20,21] and for which accurate X-ray crystallographic data are available.[29]

Here, for the first time, we provide a detailed atomistic insight into the possible reaction mechanisms that are not accessible to experimental probes. The use of the most advanced computational tools[27,28,30−34] allows us to work out free energies and provides direct evidence of the unique and cooperative catalytic role of Mg^{2+} and K^+ metal ions; the joint action of the two catalysts is found to reduce significantly the free energy barrier for the ATP hydrolysis by means of an exchange of the OH^- hydroxyl anion between the coordination shells of the two metals that otherwise would require a proton wire mechanism, shown to be energetically more demanding in a structurally similar system (actin) in which K^+ ions are not present.[23]

2. Computational Details

2.1. QM/MM Approach. In the present set of simulations, we use a first-principles quantum mechanics (QM) coupled to molecular mechanics (MM) approach (QM/MM) on the Hsc70 T13G mutant, a very reactive member of the bovine Hsc70 ATPase protein family, as provided by the Brookhaven Protein Data Bank.[29] This starting configuration, composed of the ATP Hsc70 system and the metal ions, was fully solvated, thus constructing a system of 5910 atoms plus 14 940 solvent water molecules, amounting to a total size of 50 730 atoms. We inspected the local hydrogen bond network for the closest His residues, His-89 and His-227, in order to figure out the type of protonation; as a further check, we also did a test calculation of the theoretical titration with the Poisson−Boltzmann solver as implemented in the APBS package.[35] We notice, however, that the His residues present in our Hsc70 system are not located very close to the ATP site, namely at 10.01 Å as the closest and 33.60 Å as the most distant one. Hence, the influence of His on the hydrolysis reaction is not a major issue. This T13G structure was then thermalized at room temperature for 70 ps in a box $84.13 \times 79.62 \times 75.24$ Å^3 with a classical AMBER99 force field.[30] The run was later continued to about 100 ps as a further check. The resulting equilibrated structure did not deviate significantly from the initial X-ray data, and the major contribution to the root-mean-square displacement (Figure 1a) comes from the reorganization of the solvent water. This structure was then used for the QM/MM simulations.[31,32] These were performed, within the density functional theory[36] (DFT) framework in the local spin density approximation, in terms of Car−Parrinello molecular dynamics[33] as implemented in the CPMD code.[34] HCTH gradient corrections on the exchange and correlation functional were inlcuded.[37] This particular functional has already been extensively used in several biomolecules including phosphates,[25,26,38] and its accuracy turned out to be similar to that of B3LYP. The interaction between core and valence electrons was described by Martins−Troullier pseudopotentials.[39] In the case of Mg,[38] nonlinear core corrections[40] were included, while, for K, semicore states were used.[22] Due to the inclusion of semicore states, the Kohn−Sham valence orbitals, expanded in a plane wave (PW) basis set,

(7) Senior, A. E.; Nadanaciva, S.; Weber, J. *Biochim. Biophys. Acta* **2002**, *1553*, 188−211.
(8) Dittrich, M.; Hayashi, S.; Schulten, K. *Biophys. J.* **2004**, *87*, 2954−2967.
(9) Nojii, H.; Yasuda, T.; Yoshida, M.; Kinoshita, K. *Nature* **1997**, *386*, 299−302.
(10) Böckmann, R. A.; Grubmüller, H. *Nat. Struct. Biol.* **2002**, *9*, 198−202.
(11) Dittrich, M.; Hayashi, S.; Schluten, K. *Biophys. J.* **2003**, *85*, 2253−2266.
(12) Wilbanks, S. M.; McKay, D. B. *Biochemistry* **1998**, *37*, 7456−7462.
(13) Sousa, M. C.; McKay, D. *Biochemistry* **1998**, *7*, 15392−15399.
(14) Wang, H.; Oster, G. *Nature* **1998**, *391*, 510−513.
(15) Stock, D.; Leslie, A. G. W.; Walker, J. E. *Science* **1999**, *286*, 1700−1705.
(16) Seelert, H.; Poetsch, A.; Dencher, N. A.; Engel, A.; Stahlberg, H.; Muller, D. J. *Nature* **2000**, *405*, 418−419.
(17) Smith, D. E.; Tans, S. J.; Smith, S. B.; Grimes, S.; Anderson, D. L.; Bustamante, C. *Nature* **2001**, *413*, 732−738.
(18) Palleros, D. R.; Reid, K. L.; Shi, L.; Welch, W. J.; Fink, A. L. *Nature* **1993**, *365*, 664−666.
(19) O'Brien, M. C.; McKay, D. B. *J. Biol. Chem.* **1995**, *270*, 2247−2250.
(20) Kabsch, W.; Mannherz, H. G.; Suck, D.; Pai, E. F.; Holmes, K. C. *Nature* **1990**, *347*, 37−44.
(21) Flathery, K. M.; McKay, D. B.; Kabsch, W.; Holmes, K. C. *Proc. Natl. Acad. Sci. U.S.A.* **1991**, *88*, 5041−5045.
(22) Akola, J.; Jones, R. O. *J. Phys. Chem. B* **2003**, *107*, 11774−11783.
(23) Akola, J.; Jones, R. O. *J. Phys. Chem. B* **2006**, *110*, 8121−8129.
(24) Carloni, P.; Röthlisberger, U.; Parrinello, M. *Acc. Chem. Res.* **2002**, *35*, 455−464.
(25) Gervasio, F.; Laio, A.; Iannuzzi, M.; Parrinello, M. *Chem.—Eur. J.* **2004**, *10*, 4846−4852.
(26) Gervasio, F. L.; Boero, M.; Parrinello, M. *Angew. Chem., Int. Ed.* **2006**, *45*, 5606−5609.
(27) Laio, A.; Parrinello, M. *Proc. Natl. Acad. Sci. U.S.A.* **2002**, *99*, 12562−12566.
(28) Iannuzzi, M.; Laio, A.; Parrinello, M. *Phys. Rev. Lett.* **2003**, *90*, 238302.
(29) Experimental coordinates from Brookhaven Protein Data Bank, accession number 2bup for Hsc70-T13.G mutant.
(30) Cornell, W. D.; Cieplack, P.; Bayly, C. I.; Gould, I. R.; Merz, K. M. Jr.; Ferguson, D. M.; Spellmeyer, D. C.; Fox, T.; Caldwell, J. W.; Kollman, P. A. *J. Am. Chem. Soc.* **1995**, *117*, 5179−5197.
(31) Laio, A.; VandeVondele, J.; Röthlisberger, U. *J. Chem. Phys.* **2002**, *116*, 6941−6947.
(32) Laio, A.; VandeVondele, J.; Röthlisberger, U. *J. Phys. Chem. B* **2002**, *106*, 7300−7307.
(33) Car, R.; Parrinello, M. *Phys. Rev. Lett.* **1985**, *55*, 2471−2474.
(34) CPMD; Copyright IBM Corp. 1990−2001, Copyright MPI für Festkörperforschung, Stuttgart, 1997−2004.
(35) Baker, N. A.; Sept, D.; Joseph, S.; Holst, M. J.; McCammon, J. A. *Proc. Natl. Acad. Sci. U.S.A.* **2001**, *98*, 10037−10041 (http://apbs.sourceforge.net/).
(36) Kohn, W.; Sham, L. J. *Phys. Rev.* **1965**, *140*, A1133−A1138.
(37) Hamprecht, F. A.; Cohen, A. J.; Tozer, D. J.; Handy, N. C. *J. Chem. Phys.* **1998**, *109*, 6264−6271.
(38) Boero, M.; Tateno, M.; Terakura, K.; Oshiyama, A. *J. Chem. Theory Comput.* **2005**, *1*, 925−934.
(39) Troullier, N.; Martins, J. L. *Phys. Rev. B* **1991**, *43*, 1993−2006.
(40) Louie, S. G.; Froyen, F.; Cohen, M. L. *Phys. Rev. B* **1982**, *26*, 1738−1742.

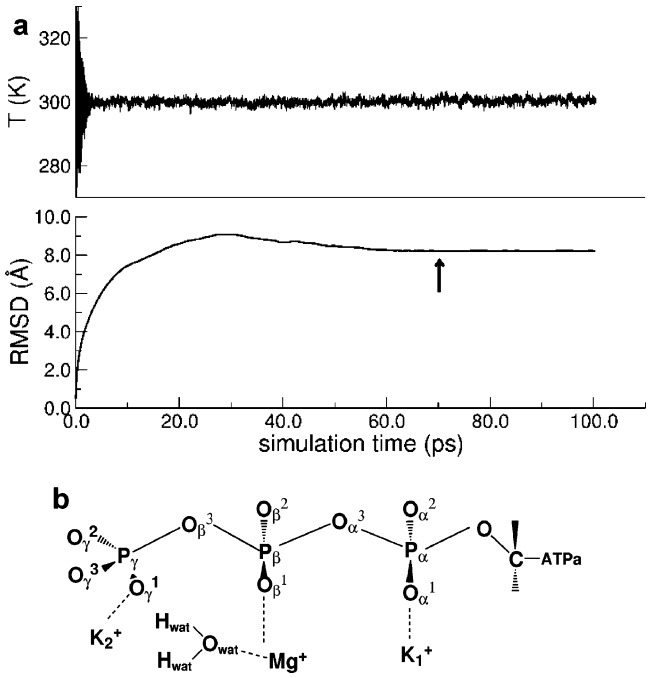

Figure 1. (a) Temperature (*T*, upper panel) and root-mean-square displacement (rmsd, lower panel) evolution during the pre-equilibration of the Hsc70 T13G mutant. The arrow indicates the 70 ps configuration used to start the QM/MM simulations. (b) Schematic view of the ATP domain of Hsc70 ATPase with standard labeling of the atoms.

required a rather large energy cutoff of 80 Ry, corresponding to 194 196 PWs and to a real space mesh of 192 × 192 × 192 points. The Brillouin zone was sampled at the Γ point only, and the QM cell size was set to 17 × 17 × 17 Å^3. This amounts to a QM subsystem of 35 atoms and 142 electrons, i.e., the three phosphates, the CH_2 group directly bound to P_α, and the two K^+ and the Mg^{2+} plus the water molecules in the related solvation shell; one capping H-like monovalent link atom was used to compensate the cut bond of the CH_2 group connecting the phosphate moiety to the MM subsystem. The QM/MM coupling adopted here is the Hamiltonian scheme that makes use of the restrained electrostatic potential (R-ESP) reported in detail in refs 31 and 32. All the CPMD runs were performed at 300 K, and the temperature was controlled via a Nosé−Hoover[41−43] chain thermostat on the ionic degrees of freedom. A fictitious electron mass of 380 au and an integration step of 4 au (0.096 fs) ensured good control of the adiabaticity.[44]

2.2. Reaction Path Sampling. The reaction path was sampled by using the metadynamics approach[27,28] by adding to the Car−Parrinello Lagrangean the degrees of freedom of selected collective variables $s_\alpha(t)$ plus a history dependent Gaussian potential $V(s_\alpha,t)$. The specific collective variables adopted in each simulation will be given in the next paragraphs, as support to the discussion. In each metadynamics run, a new Gaussian contribution was added to the penalty potential $V(s_\alpha,t)$ every $\Delta t = 0.01$ ps, amounting to 120 molecular dynamics steps, and its amplitude W_t was sampled in the interval 0.006 kcal/mol < W_t < 0.400 kcal/mol. Fictitious masses for the kinetic term of the collective variables have been set to $M_\alpha = 20.0$ au, whereas the harmonic coupling constants were set to $k_\alpha = 0.24$ au. Further details on the methods adopted here and their assessment have been explained in detail elsewhere and can be found in the cited literature.[24−26,38,45−48] The coupling of metadynamics with the QM/MM hybrid approach does not pose particular problems, since the collective variables act on the QM atoms and in this respect the method does not differ from standard full quantum metadynamics. Furthermore, this coupled scheme has already been proven to possess the ability to study with good accuracy complicated reactions in biomolecular systems.[25,26] The computational cost of the calculations presented here amounts to about 35 s per single simulation step on 16 CPUs of a Hitachi SR11000 machine. Since the local electron density used in DFT has well-known drawbacks in describing radical states, due to the incomplete cancellation of the electron self-interaction, we did some electronic structure test calculations on snapshots, extracted from the QM/MM reactive trajectory, in which OH^- and the detached P_γ-group are present using self-interaction corrections.[49] The extent of the localization of the wavefunctions and the electronic structure features did not show any noticeable difference, providing a validation to the results obtained without including self-interaction corrections.

3. Results and Discussion

3.1. Classical and Hybrid Molecular Dynamics Simulations. The detailed structure of the ATPase active site depends on the system. For instance, experiments suggest that, in both actin and F_1-ATPase, the Mg^{2+} cation adopts a bidentate configuration.[11−13,20,21] A monodentate configuration[1] seems instead realizable in Hsc70 as explained in the forthcoming discussion. A feature common to all systems is that in the ATPase moiety one Mg^{2+} cation is located between the β- and γ-phosphates and both O_β^1 and one of the three O_γ oxygen atoms are members of the first solvation shell of the cation. The solvation shell is then completed by four (bidentate case) or five (monodentate case) water molecules, thus ensuring a regular 6-fold configuration to the Mg^{2+} metal ion. Hereafter atom labeling is the standard notation adopted in the literature (Figure 1b). A still controversial question is whether Hsc70 presents a monodentate or a bidentate configuration. In the first case a fifth water molecule would be present in the vicinity of Mg^{2+}, and this additional H_2O would be the one that undergoes more easily the dissociation process that triggers the reaction. For this reason, this molecule is referred to as putative catalytic water.[13] At variance with other systems,[8] the T13G mutant of Hsc70, provided by the Protein Data Bank,[29] displays a rather high flexibility that, in turn, allows for the triphosphate chain to displace rather easily. As a consequence, O_γ atoms bonded to the terminal phosphorus atom become members of the solvation shell of a nearby K^+ (K_2^+ in Figure 2a), and this creates enough empty space to accommodate the putative catalytic water in the solvation shell of Mg^{2+}.

Indeed, in the structure of the T13G mutant derived from X-ray data,[29] the $Mg^{2+}-O_\gamma$ distance is already larger than typical $Mg^{2+}-O$ distances (∼2.10 Å) of a regular first solvation shell and the water molecules of the solvation shell have been crystallographically identified. Furthermore, we verified that even if one H_2O molecule is removed, another water molecule comes and occupies the vacant position. Hence, the monodentate configuration comes directly from the experimental evidence; thus we included all these crystal water molecules during the

(41) Nosé, S. *Mol. Phys.* **1984**, *52*, 255−268.
(42) Nosé, S. *J. Chem. Phys.* **1984**, *81*, 511−519.
(43) Hoover, W. G. *Phys. Rev. A* **1985**, *31*, 1695−1697.
(44) Grossman, J. C.; Schwegeler, E.; Draeger, E. W.; Gygi, F.; Galli, G. *J. Chem. Phys.* **2004**, *120*, 300−311.
(45) Boero, M.; Terakura, K.; Tateno, M. *J. Am. Chem. Soc.* **2002**, *124*, 8949−8957.
(46) Laio, A.; Rodriguez-Fortea, A.; Gervasio, F. L.; Ceccarelli, M.; Parrinello, M. *J. Phys. Chem. B* **2005**, *109*, 6714−6721.
(47) Ensing, B.; Laio, A.; Parrinello, M.; Klein, M. L. *J. Phys. Chem. B* **2005**, *109*, 6676−6687.
(48) Gervasio, F. L.; Laio, A.; Parrinello, M.; Boero, M. *Phys. Rev. Lett.* **2005**, *94*, 158103.
(49) VandeVondele, J.; Sprik, M. *Phys. Chem. Chem. Phys.* **2005**, *7*, 1363−1367.

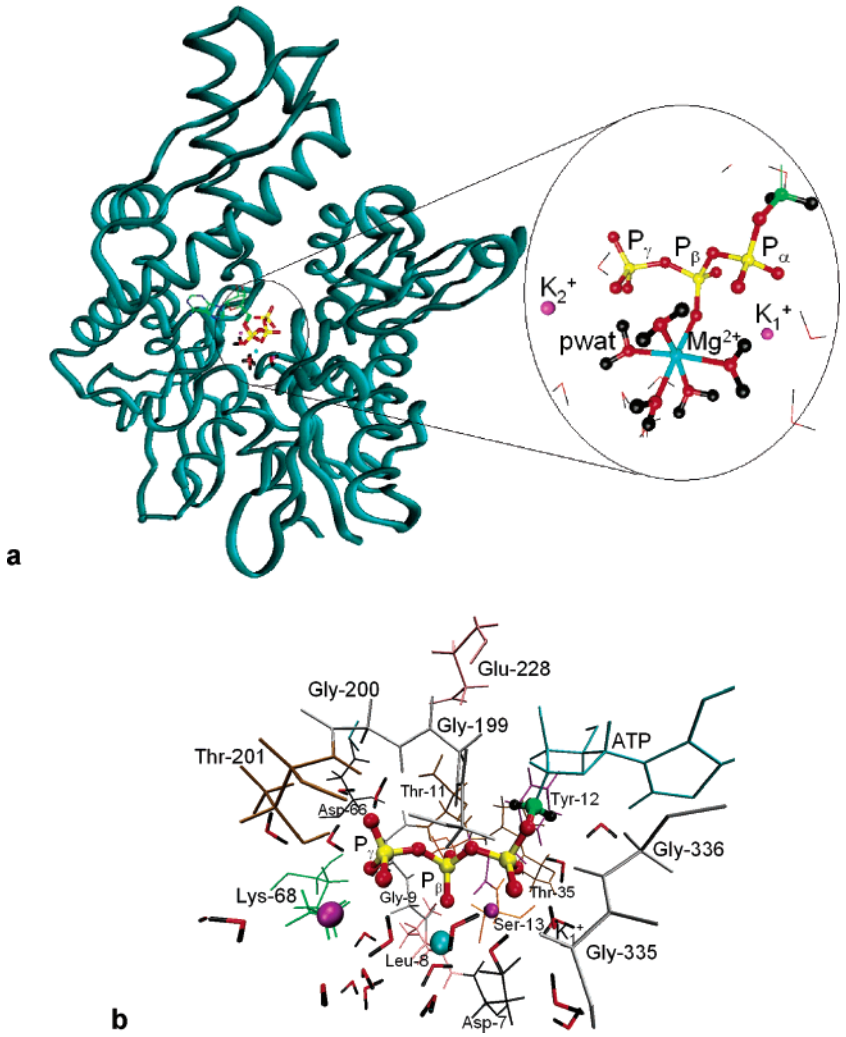

Figure 2. Hsc70 system used in the simulations. (a) Schematic view of the full Hsc70 T13G mutant and detail of the equilibrated ATP active site after 70 ns of classical dynamics and 5 ps of QM/MM dynamics. Here and in the following figures, the color code for atoms is black for H, red for O, green for C, yellow for P, cyan for Mg, and purple for K. All the classical solvent water molecules are not shown for the sake of clarity. Thick sticks and balls evidence the QM subsystem, whereas thin sticks are H_2O molecules (V-shaped) and bonds belonging to the MM part. The (QM) water molecule labeled as pwat indicates the putative catalytic water undergoing the dissociation during the ATPase hydrolysis reaction. (b) ATP site with all the residues (colored sticks) and water molecules (V-shaped red and black sticks) up to a distance of 10 Å. The color code for the residues is as follows: black = Asp, gray = Gly, brown = Thr, green = Lys, orange = Ser, purple = Tyr, light pink = Leu, dark pink = Glu. Residue labels are indicated for the sake of clarity.

pre-equilibration phase. The presence of a potassium ion in the vicinity of both Mg^{2+} and O_γ certainly contributes to the weakening or hindering of a direct coordination $Mg^{2+}-O_\gamma$, contrary to the case for actin where no K^+ metal ions are present. This T13G mutant configuration was assumed as our starting structure for a classical molecular dynamics run within the AMBER99 force field[30] for 70 ps, to pre-equilibrate the system, followed by a 5 ps QM/MM simulation to equilibrate together ionic and electronic degrees of freedom. Both the classical and the QM/MM simulations show that the monodentate coordination of Mg^{2+} with the putative catalytic water in its solvation shell is a stable configuration of the system (Figure 2a and b). Since H_2O molecules of the solvation shell and metal ions are included in the QM subsystem and since no adjustable parameters are used in our first-principles QM calculations, we can infer that the system including the putative catalytic water is not an artifact of the force field adopted. The average values of the most relevant geometrical parameters of the ATPase domain (belonging to the QM subsystem) are summarized in Table 1 and compared to the experimental data of the T13G mutant.[20,21]

Table 1. Main Geometrical Parameters of the ATPase Domain in the Hsc70 System Simulated[a]

	QM/MM	experiment
$P-O^{dangling}$ (Å)	1.50 ± 0.03	1.49−1.52
$P-O^{bridging}$ (Å)	1.59 ± 0.07	1.59−1.61
C−O (Å)	1.44 ± 0.03	1.44
POP	135° ± 4°	132°,137°
POC	120° ± 3°	121.2°
Mg−O (Å)	2.09 ± 0.11	1.99−2.13
OMgO	91° ± 6°; 174° ± 5°	83°−99°; 176°−178°
K_1-O (Å)	2.83 ± 0.07	2.79−2.85
K_2-O (Å)	2.75 ± 0.12	2.80−3.30

[a] The QM/MM values refer to the 5 ps equilibration run after 70 ps of classical Amber99 molecular dynamics simulation. The average QM/MM values are reported with their dynamical fluctuations. Experimental data are from ref 29.

The good agreement of the main geometrical parameters, averaged over the QM/MM trajectory, with the experimental structure,[29] in line with the most advanced theoretical estimations,[23] provides a sounding support to the accuracy of the approach used here. The slightly larger bond distances in the case of Mg−O are just due to the overcorrection typical of any

gradient corrected functional along with the effects of nonlinear core corrections in the pseudopotential adopted here, plus the effect due to dynamical fluctuations of the coordination shell during the run at 300 K.

3.2. Free Energy Profile, Pathway of the Reaction, and Catalytic Role of Potassium. The inspection of the reaction pathway leading to the formation of ADP was done via a set of QM/MM reactive Car−Parrinello[33,34] simulations making use of the metadynamics approach[27,28] and assuming as a starting conformation the equilibrated Hsc70 system described above. In our first simulation, we selected as a unique reaction coordinate the coordination number[28,38] of P_γ with the O atoms (O_{wat}) belonging to any water molecule in the vicinity of P_γ, i.e., $N_{coord}(P_\gamma-O_{wat})$. This choice was driven by a chemical intuition, namely, the dissociation of a water molecule $H_2O \rightarrow H^+ + OH^-$ provides the proton and the hydroxyl anion needed to start the reaction and saturate the chemical bonds of the phosphate groups that undergo the hydrolysis reaction. We acknowledge that the choice is somehow arbitrary, and for this reason, we performed three other auxiliary simulations with different reaction coordinates; these will be discussed in the next paragraphs. An analysis of the distances of the various H_2O molecules from this phosphorus atom has shown that the water molecules closest to P_γ are the ones belonging to the solvation shell of Mg^{2+}. In particular, the one that reacts with P_γ turned out to be the putative catalytic water. The evolution of $N_{coord}(P_\gamma-O_{wat})$ during the metadynamics simulation was followed until the departing inorganic phosphate group reached the border of the QM cell. The result is reported in the upper panel of Figure 3a, while the corresponding free energy profile is shown in the lower panel of the same figure. A careful check of the contribution of the last Gaussians added to the penalty potential $V(N_{coord},t)$ after the reaction was completed, and the migration of the P_i group toward the boundary of the QM cell showed that this final part adds a negligible contribution to $V(N_{coord},t)$ and that the free energy profile is substantially unaltered. This ensures the convergence of the metadynamics calculation. As a further check, we did an auxiliary longer calculation, with the same metadynamics input parameters, in which we waited for a double transition to occur. Since we are dealing with a QM cell that does not have boundary conditions, a simple continuation of the former simulation would lead to the escape of the quantum atoms beyond the QM cell boundaries. This, of course, would invalidate the whole calculation. To overcome this difficulty, we imposed on the system the restriction that QM atoms would be reflected back whenever they come too close to the QM cell walls. In practice this affects only the departing inorganic phosphate and the K^+ metal cation coordinated to it. This was implemented in a straightforward way by simply computing at each simulation step the distances of each QM atom from the cell walls. Whenever this distance was shorter than 1 Å, we reversed the sign of the momentum of that particular atom or group of atoms, $\mathbf{p}_I \rightarrow -\mathbf{p}_I$ (I = QM atom index) so that it did not go beyond the boundaries of the QM subsystem. Although artificially affecting the momentum, this does not affect the energy conservation, since momenta enter only as $\mathbf{p}_I^2$ in the total Hamiltonian.[31,32] The result of this simulation is summarized in panel b of Figure 3 and practically coincides with the former result; just a slight increase of 0.5 kcal/mol in the free energy barrier and a little broadening of the minimum on the reactant side were observed. However, due to the accuracy of DFT calculations, which is at very best 1−2 kcal/mol, and the systematic underestimation of activation energies caused by any present day exchange and correlation functionals, this difference can be regarded as negligible.

The activation barrier, estimated in terms of the free energy difference between the reactant ($N_{coord}(P_\gamma-O_{wat}) = 0.14$) and transition state ($N_{coord}(P_\gamma-O_{wat}) = 0.54$) is $\Delta F^* = 3.4$ kcal/mol, while the overall free energy of the reaction is $\Delta F = 6.9$ kcal/mol, meaning that the ADP + P_i product ($N_{coord}(P_\gamma-O_{wat}) = 0.98$) is more stable than the reactant by this amount, in rather good agreement with the experimental value[5−8,19] (7.1 kcal/mol) for the general $ATP + H_2O \rightarrow ADP + P_i$ reaction. We acknowledge that this good agreement can well be fortuitous, due to well-known problems of the exchange-correlation interaction mentioned above and affecting any DFT calculation (and extensively discussed in the related literature). Yet, comparison with available experimental data provides a sound test to the theoretical estimates.

As a further check, we estimated the total energies, i.e., the values of the DFT functional plus the ionic kinetic energies, of the initial structure and of the average configuration corresponding to the transition state at $N_{coord}(P_\gamma-O_{wat}) = 0.54$. The energy barrier in terms of total energy rises to about $\Delta E^* = 5.8$ kcal/mol, indicating a non-negligible entropy contribution including rearrangement of the solvation shells of the metal cations. As a word of warning, we stress that this high reactivity of the T13G mutant is not expected to characterize the wild type Hsc70 and might not hold for the alternative T13S mutant,[13] since conformational changes can make the scenario entirely different.

The reaction path consists of an initial dissociation of the putative catalytic water with the detached proton jumping on the closest O atom of the terminal $-P_\gamma O_3$ group and forming a stable bond, while the OH^- hydroxyl anion remains in the solvation shell of Mg^{2+} (Figure 3c). Then the $P_\gamma-O_\beta$[3] bond is cleaved (Figure 3d), and the OH^- is transferred to the departing P_γ-group forming the inorganic phosphate $H_2PO_4^-$ and leaving behind the ADP (Figure 3e). Some interesting features must be remarked upon. Namely, when the water molecule dissociates, the attacks of the proton and of the hydroxyl anion OH^- to the $-P_\gamma O_3$ group do not occur simultaneously. The first event observed in the simulation was the deprotonation of the putative catalytic water and the proton attack to the closest O_γ atom. Then, the hydroxyl anion remains close to Mg^{2+} as a member of its 6-fold solvation shell, due to the relatively strong attractive Coulomb interaction between OH^- and Mg^{2+}. In a recent simulation on an ATP model system derived from actin,[16] using a quantum approach similar to what has been used in this work, it has been shown that the propagation of H^+ and OH^- occurs via a proton wire mechanism[23] if the only metal cation present is Mg^{2+}. Conversely, K^+ alkali metal cations have shown to be essential in the activity of Hsc70.[19] The simulations presented here support this notion and show how K^+ cations can act as a powerful extra catalytic agent able to lower significantly the free energy barrier by promoting the approach of OH^- to $-HP_\gamma O_3$. Namely, the potassium ion indicated as K_2^+ is coordinated to one of the O atoms of the $-P_\gamma O_3$ group and, at the same time, is close to Mg^{2+}. As a result, in a transient configuration like the one in Figure 3d, the Coulomb repulsion

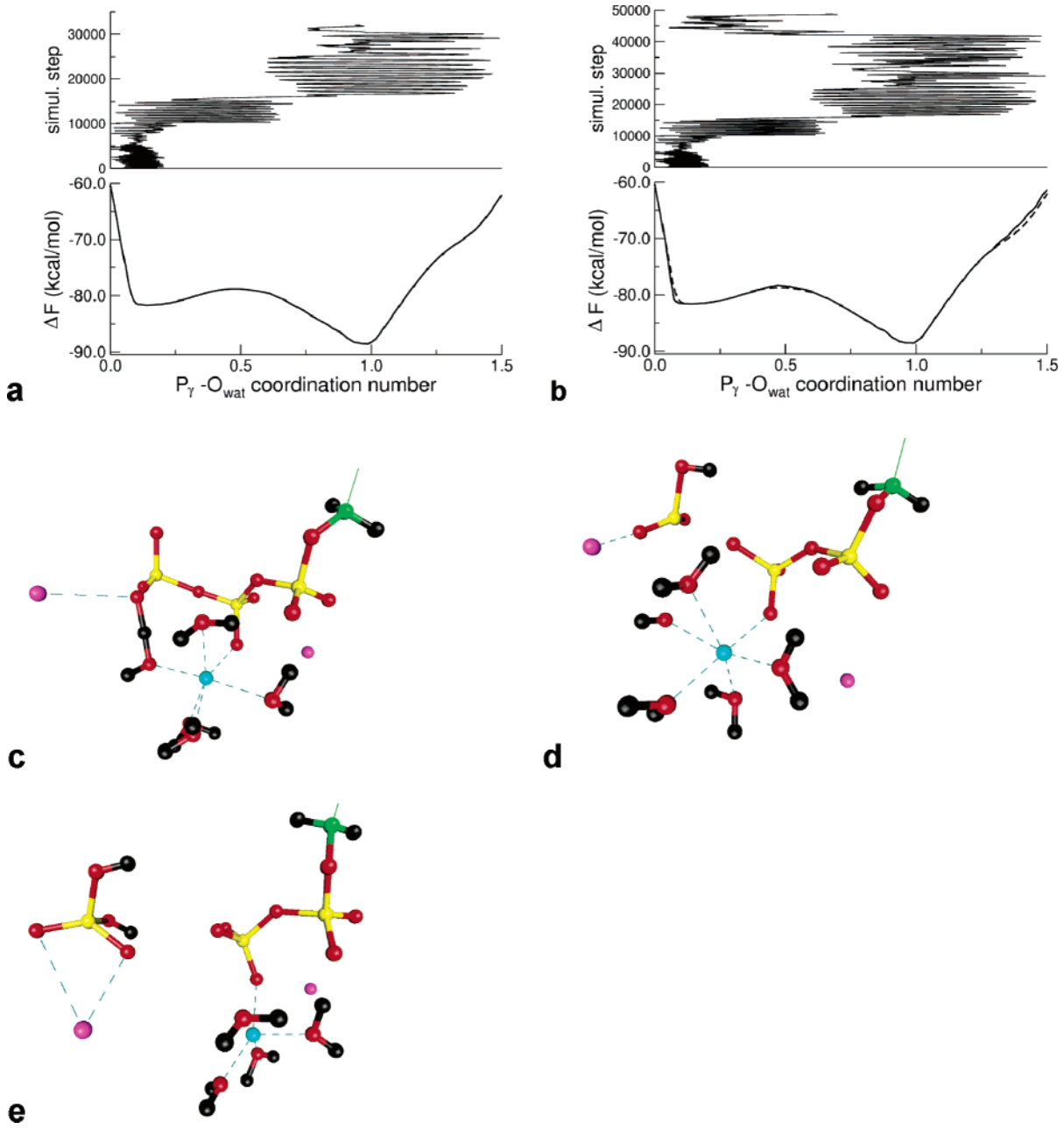

Figure 3. ATPase reaction in Hsc70. (a) Evolution of the coordination number $N_{cood}(P_\gamma-O_{wat})$ during the simulation (upper panel) and relative free energy profile (lower panel) as a function of the coordination number. The local minimum at 0.14 corresponds to the initial ATP system while the second minimum at 0.98 refers to the final ADP + P_i product. (b) Coordination number (upper panel) and free energy profile (lower panel, solid line) for the same simulation as that above including reflecting walls on the QM atoms. The superimposed dashed line is the same free energy profile of the previous panel, shown here for comparison. (c) Snapshot of the initial H^+ attack to the ATP structure upon water dissociation; (d) the transition state corresponding to the local maximum of the free energy profile around $N_{cood}(P_\gamma-O_{wat}) = 0.5$, i.e., $P_\gamma-O_\beta$[3] cleavage with the hydroxyl anion OH^- ready to react with the departing P_γ-phosphate group; (e) the final ADP + P_i product corresponding to the minimum at $N_{cood}(P_\gamma-O_{wat}) = 0.9$ of the free energy profile.

between the two metal cations K_2^+ and Mg^{2+} is partially screened by OH^-. When the leaving group $-HP_\gamma O_3$ increases its distance from the newly formed ADP moiety, the K^+ ion in the vicinity follows, bringing away in its solvation shell this OH^-. In practice, the hydroxyl anion is exchanged between the solvation shells of Mg^{2+} and K^+ (Figure 4). This replaces the proton wire mechanism evidenced in actin[23] and reduces the free energy barrier for the final transfer of the hydroxyl anion to the leaving group, leading to the formation of the inorganic phosphate $H_2P_\gamma O_4^-$. In the process, the OH^- that leaves Mg^{2+} is replaced by a (MM) H_2O molecule that approaches the metal cation and restores its 6-fold solvation shell.

This seems to be a sort of general feature common also to other biological systems: whenever a metal ion is introduced in the vicinity of an active site in solution, the hydrogen bond network of the solvent water is interrupted or broken, and thus propagation of protons and/or hydroxyl anions via a proton wire mechanism becomes hindered.[38,45] We note, also, that the departure of $H_2P_\gamma O_4^-$ with K_2^+ leaves behind the ADP with one Mg^{2+} and one K^+, as expected from experiments.[50]

3.3. An Insight into the Rate-Limiting Step and ADP Protonated State. In a second simulation we selected two

(50) Gruschus, J. M.; Greene, L. E.; Eisenberg, E.; Ferretti, J. A. *Protein Sci.* **2004**, *13*, 2029−2044.

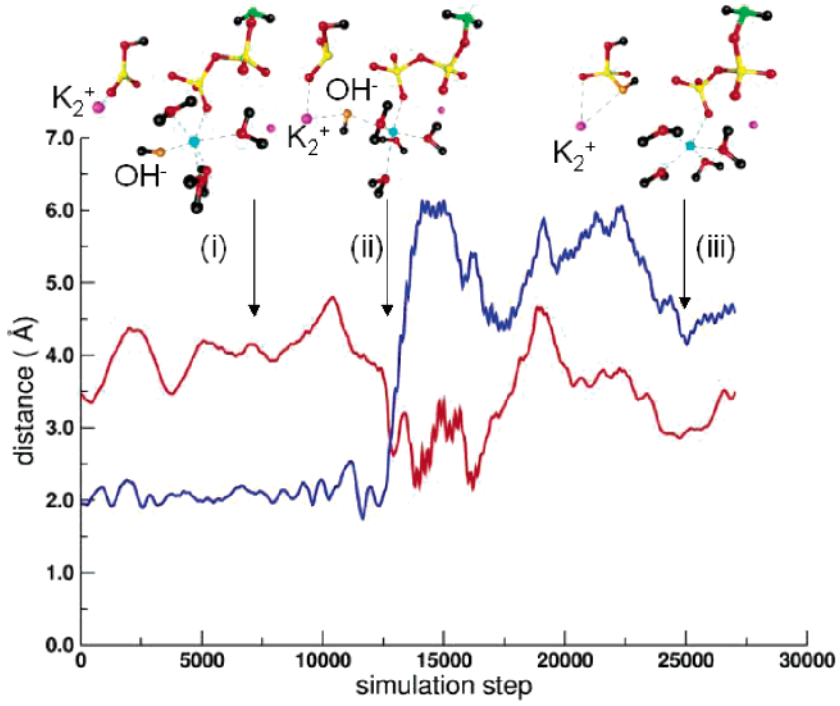

Figure 4. Evolution of the $Mg^{2+}-OH^-$ (blue line) and $K_2^+-OH^-$ (red line) distances during the ATPase reaction. The hydroxyl anion OH^- is transferred from the solvation shell of Mg^{2+} (i) to the solvation shell of K_2^+ (ii) and eventually reacts with the departing P_γ group (iii). The color code is the same as that in the previous figures apart from the O atom of the OH^- hydroxyl anion, shown in orange for the sake of clarity. The arrows indicate the approximate position of the snapshots along the trajectory.

collective variables s_α ($\alpha = 1,2$): the distance of oxygen $O_\beta{}^3$ from the hydrogen atom of the closest H_2O molecule, $s_1 = |\mathbf{R}(O_\beta{}^3)-\mathbf{R}(H_{wat})|$, and the distance of the O atom of this same water molecule from P_γ, $s_2 = |\mathbf{R}(P_\gamma)-\mathbf{R}(O_{wat})|$. The purpose was to protonate $O_\beta{}^3$ in order to see which one of the two bonds between $P_\gamma-O_\beta{}^3$ and $P_\beta-O_\beta{}^3$ would be cleaved upon the formation of a chemical $O_\beta{}^3-H$ bond. This allows us to probe whether the $P_\gamma-O_\beta{}^3$ bond cleavage observed in the former simulation was an artifact of the selected reaction coordinate or not. The results of this simulation confirmed that the previous finding was indeed correct. The QM/MM metadynamics simulation, started with these $\{s_1,s_2\}$ collective variables, has shown that initially the system explores a *valley* of local minima of the free energy surface (FES) represented by dynamical fluctuations of the solvation shell of Mg^{2+}. This is shown in Figure 5 by the ensemble of contiguous peaks ranging from $s_1 = 3.0$ Å to 5.0 Å, with s_2 values confined into the interval [3.5, 5.0] Å; the corresponding average configuration (i) is shown above the FES in the same figure. For the sake of clarity, we reversed the vertical axis, so that local minima appear as peaks in the figure. When the system overcomes these equivalent minima, the putative catalytic water dissociates into H^+ and OH^- and the detached H^+ is for a short transient time a shared proton between this OH^- and $O_\beta{}^3$, as shown by the large fluctuations of s_1 around simulation step 10 000 in Figure 6a (solid line). This transition state is the configuration labeled as (ii) in Figure 5. The system then finds a stable local minimum by forming the $O_\beta{}^3-H_{wat}$ bond shown in panel (iii) and by breaking the $P_\gamma-O_\beta{}^3$ chemical bond. This implies the overcoming of a free energy barrier $\Delta F'^* = 3.3$ kcal/mol and confirms that this is the strongest bond to be broken in the whole process, thus representing the rate-limiting step of the reaction. Indeed, by integrating out the *extra* collective variable $s_1 = |\mathbf{R}(O_\beta{}^3)-$

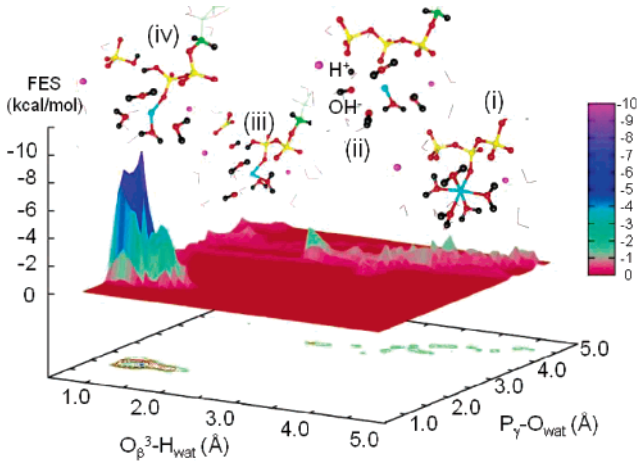

Figure 5. Free energy landscape in the space of the reaction coordinates $O_\beta{}^3-H_{wat}$ and $P_\gamma-O_{wat}$. High peaks represent local minima, since the vertical scale has been reversed for the sake of clarity. The snapshots above the free energy surface are as follows: (i) the initial ATP structure, (ii) the first transition state corresponding to the water dissociation with a detached proton (unbound black ball labeled H^+) migrating toward $O_\beta{}^3$, (iii) the second transition state with the hydroxyl anion OH^- ready to react with the departing P_γ-phosphate group, (iv) the final protonated ADP.

$\mathbf{R}(H_{wat})|$ as

$$F(s_2) = -k_B T \ln \int \exp[-F(s_1, s_2)/k_B T]\, ds_1 \qquad (1)$$

and by plotting the contribution to the free energy of s_2 only (Figure 6b) we made the remark that the ATP minima located at $P_\gamma-O_{wat} = 3.5-4.5$ Å in Figure 6b are separated by the ADP minimum around $P_\gamma-O_{wat} = 1.5$ by about 6.2 kcal/mol, accounting for the major contribution to the overall free energy difference. As in the former case, the metadynamics was

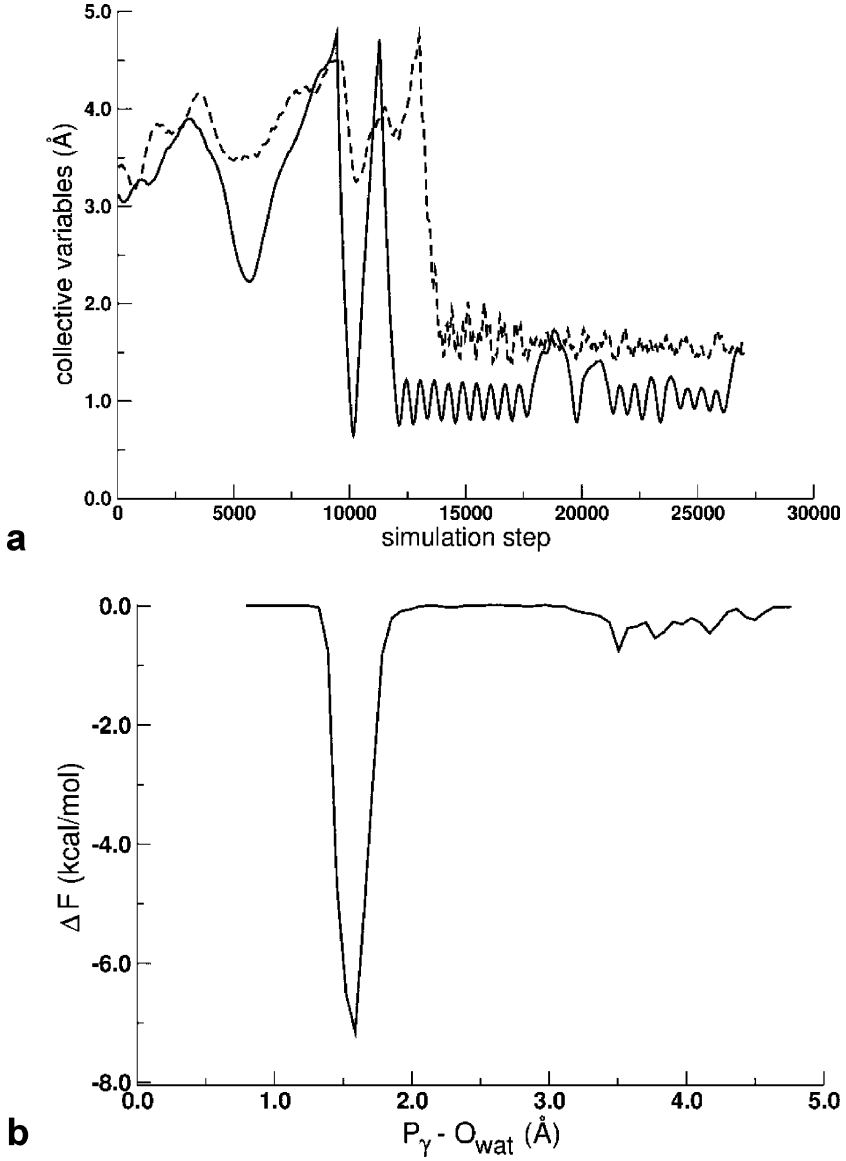

Figure 6. (a) Evolution of the two collective variables $O_\beta{}^3-H_{wat}$ (solid line) and $P_\gamma-O_{wat}$ (dashed line) during the reactive dynamics. (b) Free energy contribution relative to the $P_\gamma-O_{wat}$ reaction coordinate. Breaking the former $P_\gamma-O_\beta$ chemical bond and forming the new $P_\gamma-O_{wat}$ bond accounts for almost all the free energy barrier and represents the rate-limiting step of the hydrolysis.

continued until the leaving inorganic phosphate, after completing the reaction, reached the boundaries of the QM subsystem simulation cell. We checked the convergence of the simulation by monitoring the Gaussian contributions, observing that these did not significantly change the free energy landscape during the final part of the reaction, consisting of just a diffusion of P_i (coordinated to $K_2{}^+$) away from ADP.

Of course, constraining the system to keep the $O_\beta{}^3-H_{wat}$ bond leads to a chemically different final product, consisting of an HPO_4 departing group and a protonated ADP system. Yet, pK_a measurements coupled to conformational analyses have shown that a protonated ADP can indeed exist in Hsc70 also experimentally.[50] This reaction pathway would lead directly to the formation of the $H_2PO_4{}^-$ inorganic phosphate (and a protonated ADP) provided that the initial reactant is a protonated ATP. Thus, the result of this simulation is not just an academic speculation. It is interesting to observe that the free energy difference between the initial ATP system and the final protonated ADP + P_i product, as computed from the FES of our simulation, turns out to be $\Delta F' = 6.8$ kcal/mol, only slightly less stable than the former nonprotonated result. This finding is consistent with the experimental outcome[5−8] and supports the notion of relative abundance of protonated states.[50] Also in this case, the attack of the hydroxyl anion to the O_3P_γ group is mediated by potassium in the same way as that described in the previous section and summarized in Figure 3, underscoring the importance of both metal catalysts, Mg^{2+} and K^+, in Hsc70 ATPase.[19] The breaking of the $P_\gamma-O_\beta{}^3$ bond and its relative weakness compared to $P_\beta-O_\beta{}^3$ was confirmed by an auxiliary third simulation, started from the same initially equilibrated QM/MM structure, in which a single selected collective variable was the coordination number of $O_\beta{}^3$ with H_{wat} atoms of H_2O molecules in the vicinity and any constraint on $P_\gamma-O_{wat}$ was released. Also in this case the putative catalytic water is the H_2O molecule reacting with ATP and the bond cleavage occurs at the $P_\gamma-O_\beta{}^3$ site.

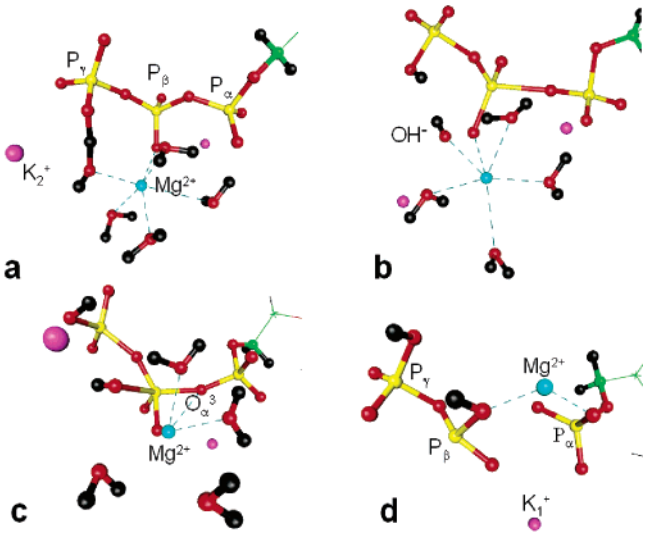

Figure 7. Main phases of the reaction at the P_β site. (a) Initial proton transfer to the $-P_\gamma O_3$ group upon water dissociation, (b) the newly formed hydroxyl anion, (c) the transition state with the disrupted solvation shell of Mg^{2+} and the metal cation approaching $O_\alpha{}^3$, and (d) the final AMP system with the detached inorganic diphosphate. The most relevant atoms have been labeled for the sake of clarity.

3.4. Hydrolysis at the P_β Site. The scenario depicted so far has shown rather clearly that the departing P_γ-group is the one binding to the OH^- provided by the water dissociation. Yet, one could argue that we biased the results by constraining in some way the P_γ atom in either the coordination number $N_{coord}(P_\gamma-O_{wat})$ or the distance $|\mathbf{R}(P_\gamma)-\mathbf{R}(O_{wat})|$. In order to dissipate any doubt, we did a fourth simulation in which the collective variables used were $s_1 = |\mathbf{R}(O_\beta{}^3)-\mathbf{R}(H_{wat})|$ and $s_2 = |\mathbf{R}(P_\beta)-\mathbf{R}(O_{wat})|$, thus releasing any constraint on P_γ and forcing the oxygen atom of the water molecule to form a new bond with P_β. This allows us to probe whether or not the final product can be $(HO_3P_\gamma-O_\beta{}^3H)^-$ plus ADP having as terminal phosphate $O_{wat}-P_\beta O_2-O_\alpha{}^3-$, contrary to all the previous results that, on the product side, present always the hydroxyl anion $HO_{wat}{}^-$ as part of the released inorganic phosphate P_i.

In this case, the simulation shows that the dissociation of the putative catalytic water and the proton attack to $O_\beta{}^3$ does not lead to a stable chemical bond. In fact, the metadynamics finds that this is just a shallow minimum and the detached proton forms a stable bond with the nearest dangling O atom of the terminal $-P_\gamma O_3$ group, as shown in Figure 7a and 7b, in a way similar to what has been found in the first simulation using $N_{coord}(P_\gamma-O_{wat})$. The reaction then becomes more problematic than all the other cases discussed above. The approach of the hydroxyl anion OH^- to P_β occurs only upon disruption and deformations of the solvation shell of Mg^{2+} while K^+ ions do not play any active catalytic role; in the process, Mg^{2+} moves toward $O_\alpha{}^3$, i.e., the oxygen atom bridging P_α and P_β, the triphosphate chain undergoes large distortions, and the potassium ion labeled as $K_2{}^+$ displaces away from the terminal phosphate. This leads to the transition state shown in Figure 7c and to a free energy barrier $\Delta F''^* = 9.2$ kcal/mol, much higher than the corresponding reactant−transition state free energy differences in all the former cases. Furthermore, the approach of a positive Mg^{2+} metal ion to $O_\alpha{}^3$ weakens the $P_\beta-O_\alpha{}^3$ bond of the five-fold P_β atom. Eventually this bond breaks producing a departing inorganic diphosphate and leaving behind an adenosine monophosphate (AMP) as sketched in Figure 7d. This is a stable minimum of the FES described by the selected collective variables, and it is located about 5.6 kcal/mol below the ATP reactant. Yet, the large displacement of the ATPase moiety, the breaking of the solvation shell of the metal cations and the absence of a concurrent catalytic role from K^+ lead to a remarkable increase of the free energy barrier, making the direct production of AMP from ATP rather unlikely.

4. Concluding Remarks

A comprehensive set of hybrid QM/MM simulations on the Hsc70 ATPase system, coupled to a dynamical computational approach for the exploration of the free energy landscape, has been performed for the first time ever in an attempt at unraveling the detailed microscopic picture of the reaction pathway leading to the formation of ADP. This represents complementary, yet fundamental, information not directly accessible to experimental probes and provides an insight into the various phases of the ATP hydrolysis common to all in this class of chaperones. We have shown how the dissociation of the putative catalytic water molecule belonging to the solvation shell of Mg^{2+} promotes the cleavage of the terminal $P_\gamma-O_\beta{}^3$ bond and how the OH^- hydroxyl anion becomes part of the departing inorganic phosphate. The catalytic role of both Mg^{2+} and K^+, inspected by simulations using different reaction coordinates, provides clear support to their peculiar cooperative action: On one hand, the approach of a positive Mg^{2+} cation to the $P_\gamma-O_\beta{}^3-P_\beta$ bridge promotes a $P_\gamma-O_\beta{}^3$ bond weakening via a partial withdrawal of electron charge in a way similar to what occurs also in other biological systems,[22,23,38,45] thus favoring the cleavage. On the other hand, a K^+ cation promotes the attack of the hydroxyl anion to P_γ cooperating with Mg^{2+} via an exchange of OH^- between the solvation shells of the two metal ions. This exchange mechanism substitutes the proton wire propagation of the OH^- hydroxyl anion found in actin[23] and contributes to the lowering of the activation barrier for the formation of the inorganic phosphate. In fact, in the absence of both the putative catalytic water and potassium cations, the total energy barrier for this process turns out to be about 10−20 kcal/mol, depending on the model system and theoretical approach used.[23,51]

We remark, in passing, that the entropy contribution is very large due to the flexibility of the triphosphate chain and the mobility of both the metal cations and the solvation water molecules. In this respect, the metadynamics approach adopted here allows us to compute directly free energy differences ($\Delta F = \Delta E^{tot} - T\Delta S$) relevant to the pure chemical reaction, a quantity that would be difficult to extract from the total energies E^{tot}. Finally, we have given an insight into the relative bond strength of the terminal $P_\gamma-O_\beta{}^3-P_\beta$ bridge and in the rate-limiting step of ATP hydrolysis in Hsc70. These auxiliary simulations, useful in exploring the phase space spanned by different reaction coordinates, allowed us also to inspect a protonated state of ADP and the formation of AMP. In the former case, free energy barriers and overall ΔF close to the ones for the unprotonated ADP turned out to be in qualitative agreement with conclusions inferred on the basis of pK_a measurements and related structural analyses.[50] In the latter case,

(51) Grigorenko, B. L.; Rogov, A. V.; Nemukhin, A. V. *J. Phys. Chem B* **2006**, *110*, 4407−4412.

we have shown how the direct formation of AMP from ATP is energetically more demanding due to large conformational changes in the triphosphate chain, lack of any active catalytic role of K^+, disruption of the solvation shell of Mg^{2+}, and consequent displacement of the metal cation. A rough estimation of the rate constant ratio between ADP ($k_{ATP-ADP}$) and AMP ($k_{ATP-AMP}$) formation can be expressed in terms of a ratio of Boltzmann factors, and using our computed free energy barriers, we get $k_{ATP-ADP}/k_{ATP-AMP} \approx \exp(-\Delta F^*/k_BT)/\exp(-\Delta F''^*/k_BT) = 8 \times 10^3$, indicating that the direct production of AMP is highly improbable.

Acknowledgment. We gratefully acknowledge fruitful discussions with M. Parrinello, F. L. Gervasio, A. Laio, M. Iannuzzi, M. Tateno, K. Kamiya, and A. Ubaldini. Computations were done at the Science Information Processing Center, University of Tsukuba, High Performance Computing System, Hokkaido University, and JAEA Supercomputer Facility. M.B. acknowledges the JST-CREST project and Grant in aid No. 18054004 of MEXT.

JA064117K